Nickel Complexes and Carbon Dots for Efficient Light-Driven Hydrogen Production

Kalliopi Ladomenou, Michael Papadakis, Georgios Landrou, Michel Giorgi, Charalambos Drivas, Stella Kennou, Renaud Hardré, Julien Massin, Athanassios Coutsolelos, Maylis Orio

FULL PAPER

Nickel complexes and carbon dots for efficient light-driven hydrogen production

Kalliopi Ladomenou,*[a] Michael Papadakis,[b] Georgios Landrou,[a] Michel Giorgi,[c] Charalambos Drivas,[d] Stella Kennou,[d] Renaud Hardré,[b] Julien Massin,[b] Athanassios G. Coutsolelos,*[a] and Maylis Orio*[b]

Abstract: Nitrogen-doped carbon dots were used as photosensitizers for H_2 evolution in the presence of a series of mononuclear thiosemicarbazone nickel complexes. The catalysts were designed to display different substituents at the para position of the phenyl rings. These chemical modifications tune the electron-donating abilities of the complexes and influence their capability to reduce protons into hydrogen. All photocatalytic experiments were performed in aqueous solution, using as sacrificial electron donor TCEP/Asc (1:1), 0.1 M each, at pH=5. The complex bearing the most electron-donating ligand with the dimethylamino ($N(CH_3)_2$) substituent behaves as the best catalyst in our series of photocatalytic systems with TON_{CAT} = 148, under white led radiation for 30 h. Therefore, this noble metal-free system can effectively produce hydrogen in water and further chemical modification of the ligand will likely improve its production.

Introduction

Clean and renewable energy production is part of many recent studies all over the world. It is vital to develop new technologies since the combustion of fossil fuels is strongly related to global warming and climate change due to the production of greenhouse gases such as CO_2. A reaction able to provide a solution to the above issue is the photochemical water splitting with the production of H_2.[1-2] Hydrogen is considered an ideal solar gas since it can easily produce a large amount of energy and, upon its combustion, it does not produce any harmful products.[3]
The photochemical hydrogen production process mimics natural photosynthesis and the key challenge of this process is the efficient development of catalysts able to produce hydrogen from protons.[4-5] Also, this approach requires materials able to absorb light and carry out charge separation resulting in the presence of electrons on one side and holes on the other site. These charge-separated states must be stable enough to drive the chemical reaction towards effective hydrogen production.[6-7]

[a] Dr. K. Ladomenou, G. Landrou, Prof. A. G. Coutsolelos
Laboratory of Bioinorganic Chemistry, Chemistry Department,
University of Crete, PO Box 2208, 71003 Heraklion, Crete, Greec
E-mail: kladomenou@uoc.gr, acoutsol@uoc.gr
http://www.chemistry.uoc.gr/coutsolelos/
[b] M. Papadakis, Dr. R. Hardré, Dr. J. Massin, Dr. M. Orio
Aix Marseille Univ, CNRS, Centrale Marseille, iSm2, Marseille, France
E-mail: maylis.orio@univ-amu.fr
https://ism2.univ-amu.fr/fr
[c] Dr. M. Giorgi
Aix Marseille Univ, CNRS, Spectropole FR1739, Marseille, France
[d] Dr. C. Drivas, Prof. S. Kennou
Surface Science Laboratory, Chemical Engineering Department,
University of Patras, 26504 Patras, Greece

Supporting information for this article is given via a link at the end of the document.

Promising light-harvesting materials are carbon dots as they feature efficient electron transfer properties and photostability. They are noble metal-free and are synthesized with low-cost preparation techniques on a large scale.[8-11] These types of light harvesters have already been used for hydrogen production by our group and others, and they produce promising results, despite the limited number of studies that have been performed.[12-13] On the other hand, it is important to use appropriate catalysts that can efficiently produce hydrogen. In the last decade, a plethora of first-row transition metal complexes based on Co, Ni, Cu, Fe, and Mo have been developed towards H_2 evolution.[14-19] Many photocatalytic systems that use molecular catalysts coupled with a wide range of different photosensitizers have been reported in the literature. They can catalyze the visible light-driven hydrogen evolution and produce an efficient amount of hydrogen but they often lack prolonged stability upon their irradiation.[20-25] Among these catalysts, we can distinguish Ni-based complexes with thiosemicarbazone ligands.[26-30] These type of ligands have already been studied and proved to be redox-active.[31-39] Furthermore, the presence of S- and N-atoms in the ligand permits the protonation of the ligand and can serve as proton relays.[40-42] In the literature there are two examples that uses a nickel(II) thiosemicarbazone complex as a catalyst able to produce H_2 upon photo irradiation. In the first example the catalyst is placed on a Si surface.[29] In the second example the same catalyst was used with CdS nanorods as a photosensitizer.[30] The system after irradiation in the visible light was able to produce H_2 using ascorbic acids as sacrificial electron donor (SED). The authors mentioned that the photosensitizer and the catalyst were stable upon light irradiation, but the ascorbic acid decomposed. Therefore, the combination of these type of nickel complexes with other materials such as carbon dots as light harvesters produce a very promising system for effective hydrogen evolution. Moreover, it is not yet clear what is the effect of the chemical nature of the ligand on the activity of thiosemicarbazone-based catalysts. Thus, we decided to explore the influence of the presence of an electron-donating or an electron-withdrawing group located at the para position of the phenyl ring. In a recent study, no correlation between the presence of electron-donating groups of the same ligand and the resulting electrocatalytic H_2 production could be extrapolated.[28] More specifically, the most electron-donating group $N(CH_3)_2$ exhibited a turnover number (TON) of 10, whereas the least electron-donating group CN mediated a TON of 8. Since, as far as we know, there are no other examples in the literature that examined the structure-activity relationship in such nickel-based catalysts, it is important to study such structural effect of the catalysts in the context of hydrogen photo-production. In this regard, the only catalysts that have been studied are polypyridine cobalt(II) complexes in tetradentate, pentadentate, and hexadentate ligands, bearing electron-donating and electron-withdrawing groups in different positions.[43-47] The results of these

studies indicated that it remains unclear how the modification of the ligand might affect the activity of the catalysts.

Herein, we present the study of a photocatalytic hydrogen evolution system consisting of two types of carbon dot materials as light harvesters in combination with six different thiosemicarbazone nickel complexes as molecular catalysts. More specifically, the light-harvesting materials are carbon dots (**Cdot**) and nitrogen-doped carbon dots (**NCdot**) (Figure 1). The molecular hydrogen evolution catalysts are nickel(II) based complexes with thiosemicarbazone ligands bearing different types of substituents, namely **NiN(CH$_3$)$_2$**, **NiN(CH$_3$)$_2$CN**, **NiSCH$_3$**, **NiOCH$_3$**, **NiCN**, **NiPh** (Figure 1), whose synthesis was described in our previous work.[27-28] This set of complexes also includes a new catalyst in our series, **NiPh** (see Supporting Information for details).

The hydrogen production is studied in aqueous solution with the use of a sacrificial electron donor (SED), tris(2-carboxyethyl)phosphine/ascorbic acid (TCEP/Asc) 0.1 M each in a (1:1) ratio at pH=5, under white led irradiation. This synthetic approach benefits from easy preparation and modification of the catalysts by adding different electron-donating groups at the para position of the phenyl ring of the thiosemicarbazone ligands. In addition, the use of carbon dots exhibits several advantages such as ease and low-cost preparation of the light-harvesting material, making the whole system very promising for hydrogen production. In this report, the photocatalytic hydrogen production experiments were optimized. Fluorescence spectroscopy studies were performed to elucidate the reaction mechanism of our system in the presence of carbon dot at different concentration of nickel catalysts.

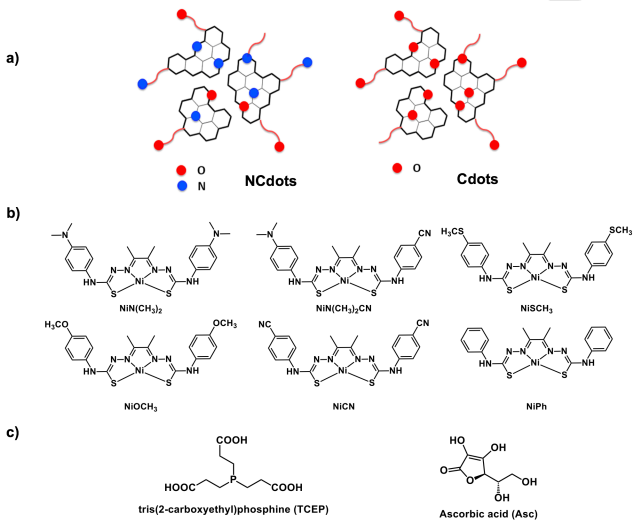

Figure 1. Chemical structures of a) carbon dots, b) Ni catalysts and c) SED.

Results and Discussion

Synthesis and characterization of carbon dots. The preparation of carbon dot materials was done according to our previous published work.[12] To extend the characterization of these photosensitizers, we performed ^{1}H-NMR and X-ray photoelectron spectroscopy (XPS) analysis. As shown in Figure S8, the ^{1}H NMR signals of the starting materials of carbon dots, namely citric acid and ethylenediamine, are not present in the **NCdot** spectrum, whereas proton signals are present in the range from 6.2 to 1.0 ppm.

XPS analysis was done to identify the elemental composition and the type of chemical bonds that are present in carbon dot materials (Figure 1). The samples, named **Cdot** and **NCdot**, were pressed as received onto thick Pb sheets to be introduced into the ultra-high vacuum chamber. XPS measurements were carried out using unmonochromatized Al Ka line at 1486.6 eV (12 kV with 20 mA anode current) and a Leybold EA-11 analyzer with a constant pass energy of 100 eV. The analyzed area was approximately a 2x5 mm^2 rectangle, positioned near the geometric center of each sample. XPS analysis was carried out at a 0 degrees take-off angle (normal to the sample area). In all XPS spectra, the Binding Energy (BE) of the C-C bond of the C 1s peak at 284.8 eV was used as a measured BE reference.

From the wide scan survey spectra (not shown), the photoelectron peaks of C and O were detected for all the samples, as well as N for the **NCdot** sample and Na for the **Cdot** one. A small amount of Pb from the Pb sheet was also present. Detailed scans of the most prominent photoelectron peak of each element present, as well as the Na Auger region, were taken to have an insight into their chemical state. Quantitative analysis was done after the area of the peaks was measured upon utilizing a Shirley background, as summarized in Table S4.

In Figure 2, the C 1s region is shown for the two samples. For both, spectra deconvolution was done to discern the different chemical species. The fitting was done constraining the position of the peaks to be ±0.2 eV of reported values and the full width at half maximum (FWHM) to be equal among them. Also, the areas of the C-N and COONa peaks were correlated with the area of the N 1s and Na 1s spectra respectively. For both spectra, the most prominent peak at 284.8 binding energy (BE) is attributed to C-C bonds from the carbon dots. At higher BEs, there are the different C bound to O species, namely the C-O group at 286.4±0.2 eV, the C=O one at 287.9±0.2 eV, and the COOH one at 289.2±0.2 eV.[48] These functional groups originate from the thermal decomposition of the precursors and possible oxidation from the ambient environment when handled. Additionally, for the **Cdot** sample, another peak was used for the COONa group at 288.0±0.2 eV,[49] and for the **NCdot** sample, the peak at 285.7±0.2 eV corresponds to C-N species.[48]

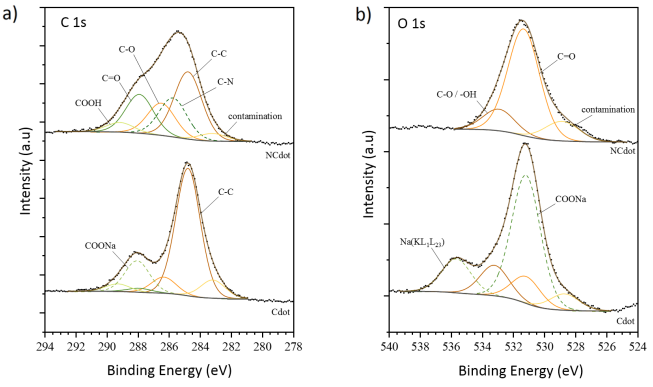

Figure 2. XPS spectra of the a) C 1s and b) O 1s regions together with their deconvolution for all the samples. Dashed lines represent the unique species of each sample.

Similar to the C 1s region, deconvolution for the O 1s region (Figure 2b) was done using the same constraints. The oxygen species used for the deconvolution were C=O (531.3±0.2 eV), C-O/-OH (533.1±0.2 eV),[48] and COONa (531.2±0.2 eV).[50] At 535.7±0.1 eV, there is also the Na KL_1L_{23} Auger photoelectron peak. At both C 1s and O 1s deconvolutions, another peak at low BE was used, named contamination, which is from the Pb sheet and was not taken into account. Their positions and relative intensities are summarized in Table S5.

Figure S9 shows the N 1s region for the **NCdot** sample. A single peak can be seen at 400.3±0.1 eV and is attributed to C-N-H bonds.[51] The XPS spectra of the Na 1s and Na $KL_{23}L_{23}$ regions are shown in Figure S10. A single peak can be seen for the Na 1s and is located at 1071.5±0.1 eV. For the accurate identification of the Na functional group, the modified Auger parameter was estimated as the sum of the binding energy of the photoelectron peak and the kinetic energy of the Auger peak, which is found to be 2061.3±0.2 eV, is attributed to COONa.[49]

Photocatalytic H_2 production. In our recent work, we described the synthesis of carbon dots (**Cdot**) and nitrogen-doped carbon dots (**NCdot**) as well as their physical and structural characterization.[12] In addition, we studied the ability of these materials to evolve H_2 production quite efficiently with the use of molecular cobalt catalysts. Therefore, we wanted to extend our previous effort by using the carbon dot materials with different transition metal-based catalysts. In this study, we thus performed hydrogen evolution experiments using these two types of carbon dots in combination with a series of Ni thiosemicarbazone catalysts which display different groups at the para position of the phenyl ring of the ligand. Our initial photocatalytic hydrogen evolution efforts proved unproductive, thus are presented in detail at the supporting information section. The most successful photocatalytic system was the one that used **NCdot** as photosensitizer, a mixture of 0.1 M each, TCEP/Asc (1:1) as SED at pH=5 and a white led as a light source. When **Cdot** was used as photosensitizer, no hydrogen could be detected, possibly due to the better charge transfer of **NCdot**, since the presence of nitrogen produce a material with n-domains as already have been mentioned by us and others.[9, 12, 52] The presence of C-N species in nitrogen doped carbon dots are shown with XPS analysis of the material.

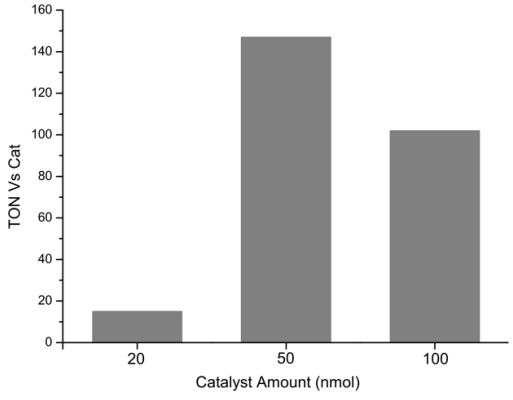

Figure 3. Photocatalytic hydrogen production plots of 10 mg NCdots in three different amounts of the catalyst **$NiN(CH_3)_2$**: 20, 50 and 100 nmol. The photocatalytic experiments were conducted in aqueous TCEP/Asc (1:1) 0.1 M each at pH = 5. All the results presented in the hydrogen production plots are the average values of three independent measurements (within 5-10% error).

In order to optimize the best catalyst's concentration various quantities 20, 50, and 100 nmol were used keeping constant the amount of photosensitizer (10 mg) as shown in Figure 3. The maximum performance of 148 TON was reached when 50 nmol of the catalyst **$NiN(CH_3)_2$** was used. Then, we performed the catalytic experiments with all six Ni catalysts and the results are presented in Figure 4. Most of the photocatalytic reactions reached a plateau after about 30 h of white led irradiation.

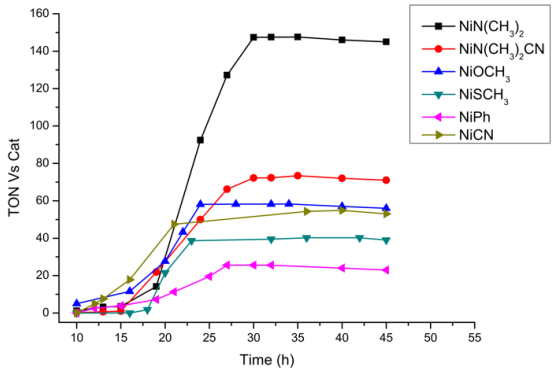

Figure 4. Photocatalytic hydrogen production plots of 10 mg **NCdot** with 50 nmol nickel catalysts: **$NiN(CH_3)_2$**, **$NiN(CH_3)_2CN$**, **$NiSCH_3$**, **$NiOCH_3$**, **NiCN**, **NiPh**. All photocatalytic experiments were performed in aqueous TCEP/Asc (1:1) 0.1 M each at pH = 5. All the results presented in the hydrogen production plots are the average values of three independent measurements (within 5-10% error).

The highest turnover number (TON) TON_{CAT} = 148 was obtained with the **$NiN(CH_3)_2$** catalyst and the minimum TON_{CAT} = 26 with **NiPh**. The TON_{CAT} values obtained with the other catalysts range between these two extreme values. More specifically, the measured TON_{CAT} values are 58, 55, and 40 for **$NiOCH_3$**, **NiCN,** and **$NiSCH_3$**, respectively. The H_2 production performances suggest that the different substitutions of the ligands affect the photocatalytic ability of the system. From these measurements, one can observe that the electron-donating ability of the para substituents ($N(CH_3)_2$ > NCH_3CN > OCH_3 > SCH_3 > Ph > CN) does not follow the light-driven H_2 production performances (Figure 5).

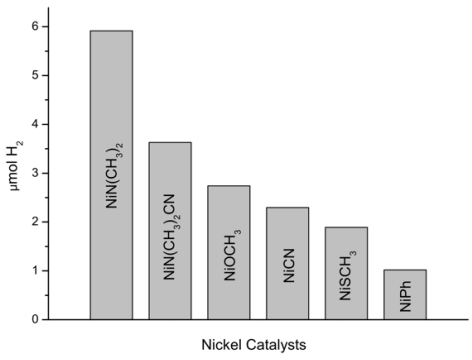

Figure 5. Photocatalytic hydrogen production (µmol H_2) upon irradiation of 10 mg **NCdots** in the presence of 50 nmol of various nickel catalysts in aqueous TCEP/Asc (1:1) 0.1 M each at pH = 5. All the results presented in the hydrogen production plots are the average values of three independent measurements (within 5-10% error).

Interestingly, a similar conclusion was reached for a series of cobalt polypyridine complexes recently reported in the literature. In this study, the authors concluded that the most dominating factor for effective photocatalysis was the position of the substituent and not its chemical nature.[44]

Additionally, control experiments were done in the absence of the **NiN(CH$_3$)$_2$** catalyst, in the absence of the **NCdot** photosensitizer, in the absence of TCEP/Asc, and in the dark. In any case, no H_2 was produced which indicates that all components are essential for H_2 production in our system. To exclude the presence of Ni nanoparticles due to the degradation of the catalyst, mercury poisoning experiments were performed. Photocatalytic experiments in the presence of mercury showed no change in H_2 production (TON_{CAT} = 135), thus confirming the stability of the catalyst upon photocatalytic reaction. Moreover, when 50 nmol of $NiCl_2$ was used as an alternative to the Ni molecular catalysts, no H_2 was evolved, supporting the essential role of Ni complexes as catalysts. Regeneration experiments were done upon photobleaching of the photosensitizer, 10 mg of carbon dots were added and the system started producing H_2.

In these photocatalytic systems, H_2 production was detected after about 13 h of irradiation for all catalysts. This was also the case in our previous work, where under similar conditions H_2 production was observed after 10 to 15 hours.[12] The only difference was the light source and the molecular catalyst. Since, in this report the delay in H_2 detection was similar for all nickel catalysts, we thought to investigate the photosensitizer. For that reason, we irradiated 10 mg of **NCdots** in the presence of SED for 13 h and we measured the quantum yield (QY) which was 16 % compared to the initial material with QY=26 %. The XRD pattern of the material before and after light irradiation showed no difference (Figure S12). In addition, we collected TEM images before and after irradiation (Figure 6). The images show that, after light irradiation, the material retains its spherical morphology but the diameter of some particles is much bigger (Figure 6 c and d) compared to the carbon dots before irradiation (Figure 6 a and b). Consequently, upon light irradiation, the morphology of the material changes, and possibly must obtain a specific form in order to start producing H_2.

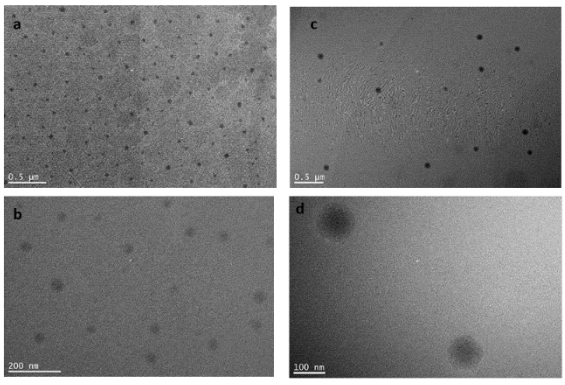

Figure 6. TEM images of **NCdots** before light irradiation (a and b) and after 12 h of white led irradiation (c and d).

In order to prove that the transformation of the photosensitizer is done exclusively upon light irradiation we stirred all components of our best photocatalytic system in the dark overnight. Then, we started the irradiation of the system with a white led. Once again, the system started producing H_2 after about 10 h of irradiation and reached 132 TON_{CAT} after 30 h, which is similar to our best system (148 TON_{CAT}).Therefore, light irradiation is responsible for the transformation of the photosensitizer and this alteration is important for the carbon dots to absorb light and finally produce H_2. In order to study the performance of our system concerning the delay of hydrogen production, we first irradiated the photosensitizer with the SED for 13 h. Then we added **NiN(CH$_3$)$_2$** catalyst and the mixture was purged with nitrogen for 15 min in order to remove oxygen, Next, after 5 h of irradiation the system started producing H_2 and a reached a plateau (TON_{CAT} = 135) after 20 h (Figure S13). Therefore, our photocatalytic system work faster if we pre-irradiate just the photosensitizer and then add the catalyst.

Photocatalytic mechanism. The thermodynamic ability for photochemical hydrogen evolution was evaluated by measuring the redox potentials of all nickel catalysts and the **NCdot** photosensitizer (Table 1). The valence band (VB) and the conduction band (CB) of nitrogen-doped carbon dots were calculated in our previous work.[12] The redox potentials of nickel catalysts were recorded in anhydrous DMF as listed in our recent report.[28] Based on all these values, the ΔG (PS/Cat) were calculated for all the catalysts and the resulting negative potentials nicely explain the photocatalytic activity of all nickel catalysts From the measured data, it is obvious that hydrogen production is thermodynamically allowed for all the catalysts used in these systems.

Furthermore, photoluminescence experiments were performed (Figures S14-S19) to clarify the mechanism of the photocatalytic reaction. The emission experiments were performed with a constant amount of **NCdots** in the presence of various concentrations of nickel catalysts and using water as solvent.

Table 1. Redox potentials (eV vs. NHE) of the photosensitizer and catalysts with the thermodynamic driving forces of electron transfer processes ΔG_1 (PS/Cat) and ΔG_2 (PS/Cat) (eV).

Compounds	E_{VB}[a]	E_{CB}[b]	E_{00}[c]	
NCdot	1.01	-2.13	3.14	
	$E_{1/2,1}$[d]	$E_{1/2,2}$[d]	ΔG_1 (PS/Cat)	ΔG_2 (PS/Cat)
NiN(CH$_3$)$_2$	-0.99	-1.48	-1.14	-0.65
NiN(CH$_3$)$_2$CN	-0.85	-1.46	-1.28	-0.67
NiSCH$_3$	-0.87	-1.50	-1.26	-0.63
NiOCH$_3$	-0.94	-1.57	-1.19	-0.56
NiCN	-0.77	-1.36	-1.36	-0.77
NiPh	-0.99	-1.67	-1.14	-0.46

[a] Oxidation potentials were measured by cyclic voltammetry and were referenced to NHE by addition of +0.193V. [b] Values were calculated as the difference of the oxidation potentials and the optical band gap energy E_{00}, calculated in eV. [c] E_{00} values were calculated form the intersection between the normalized absorption and emission spectra. [d] Reduction potentials were measured by cyclic voltammetry and were referenced to NHE.

Each catalyst was dissolved in a concentrated solution of DMSO, from which various amounts of catalysts were added including the concentration used for the photocatalytic experiments. Then, the emission spectra were monitored upon excitation at 340 nm and in all cases, the emission intensity was significantly decreased up to more than 90 %. Only in the case of **$NiOCH_3$** and **$NiN(CH_3)_2CN$** catalysts, the quenching was about 75 % and 85 %, respectively. Next, the Stern-Volmer and quenching constants were calculated according to the literature (Table 2), the fitting curves were generated (Figures S20-S25) and the values of the ascorbic acid were obtained from our previous work.[12]. For all catalysts, the K_{sv} is much bigger compared to ascorbic acid (K_{sv} = 13.8) and the quenching constants of all catalysts (K_Q = 1.1 x 10^{12} - 9.0 x 10^{12}) are greater compared to the SED's one (K_Q = 1.3 x 10^9).

Table 2. Stern-Volmer constant K_{sv} and quenching constant K_Q of all nickel catalysts.

	K_{sv} (M^{-1})	$K_Q=K_{sv}/\tau$ ($M^{-1}s^{-1}$)
$NiN(CH_3)_2$	43574	4.1 x 10^{12}
$NiN(CH_3)_2CN$	21128	2.0 x 10^{12}
$NiSCH_3$	94414	9.0 x 10^{12}
$NiOCH_3$	11726	1.1 x 10^{12}
NiCN	52555	5.0 x 10^{12}
NiPh	63313	6.0 x 10^{12}
Asc	13.8	1.3 x 10^{12}

Under our photocatalytic experimental conditions using 0.1 M of SED and 16 µM of each catalyst, the quenching is more pronounced in the case of ascorbic acid. Consequently, the photoinduced electron is transferred from the ascorbic acid to the CB of carbon dots (reductive quenching), since the concentration of the SED is much greater compared to the catalyst's one.
A summary of all the above experimental studies leads us to propose a possible mechanism of H_2 evolution as shown in Scheme 1.

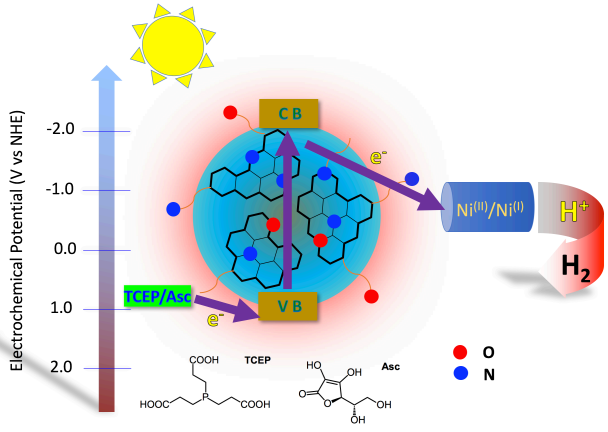

Scheme 1. Photocatalytic mechanism for H_2 evolution using nitrogen-doped carbon dots as photosensitizer, TCEP/Asc as sacrificial electron donor and Ni complexes as catalysts.

Upon photoexcitation of carbon dots by visible light irradiation, the electrons are transferred to the CB. The hole that is formed in the VB of the photosensitizer is filled by an electron transferred from the SED via a reductive quenching process. The photogenerated electrons are then transferred to nickel catalysts, which are subjected to subsequent protonation and reduction steps following a ligand-assisted metal-centered pathway and leading to the formation and release of H_2.[53]

Conclusion

The present study reports the performances of new photocatalytic hydrogen evolution systems composed of carbon dot materials and a series of noble metal-free complexes. While nitrogen-doped carbon dots are employed as light harvesting materials, nickel complexes with redox active ligands play the role of catalytic centers. The latter correspond to a series of thiosemicarbazone complexes for which the phenyl ring substituents were chosen to cover a wide range of electron-donating properties. This synthetic design was meant to modulate the electronic properties of the catalysts based on the different Hammett Sigma constants at the para position of the benzene groups. We evaluated the photocatalytic capability of the resulting systems to promote hydrogen evolution in aqueous solution, in the presence of a sacrificial electron-donor and under light irradiation. The conditions of the photoreaction were optimized to determine the parameters affecting the hydrogen evolution experiments (i.e. irradiation type, SED nature, catalyst concentration and nature, and ratio). This allowed us to probe the most efficient photocatalytic system, which was found to be the **NCdots** associated with the **$NiN(CH_3)_2$** catalyst with a calculated TON of 148 when using a TCEP/Asc (1:1) mixture at pH=5 and under white led radiation for 30 h. Our results indicate that the chemical nature of the substituent in the para position of the ligand indeed influences the photocatalytic behaviour of the systems and their hydrogen evolution performances. However, consistently with our previous study on the electrocatalytic performances of these complexes, it remains difficult to find a clear rational between the catalysis parameters, i.e. the TON values, and the electron-donating ability of the substituents ($N(CH_3)_2$ > NCH_3CN > OCH_3 > SCH_3 > Ph > CN). Recent reports on cobalt complexes suggest that the position of the substituent rather than their chemical nature might be a key element to better control and understand the photocatalytic reaction. Hence, this encourages us to pursue the current work in our group on chemically-modified thiosemicarbazone nickel complexes to decipher the key elements that control their catalytic capabilities and improve their performances for both electro- and photoproduction of hydrogen.

Experimental Section

General. All reagents and solvents were purchased from usual commercial sources and used without further purification, unless otherwise stated. The synthesis of **NCdot** were reported in detail in our previous work.[12] The nickel thiosemicarbazone complexes were prepared according to procedures previously described and their characterizations were also reported.[27-28] The alternative synthesis and full characterization of the complex **NiPh** are described in the Supplementary Information (Figures S1-S7 and Tables S1-S3). CCDC numbers 208130, 2081301 and

2081302 c contains the supplementary crystallographic data for this paper. ^{1}H NMR spectra of the compounds were recorded on Bruker AMX-500 MHz and Bruker DPX-300 MHz spectrometers. The solution of the sample was in deuterated solvent by using the solvent peak as the internal standard. X-Ray powder diffraction (XRD) Bruker Model D8 equipped with twin-twin technology, Geometry 2theta/theta. A transmission electron microscopy (TEM) system (Model JEM-2100F electron microscope (JEOL, Japan)) was used for morphology characterization of C-Dots. A dilute carbon dot stock solution was deposited onto the grid for subsequent HRTEM imaging, using an 80 kV accelerating voltage. High-resolution mass spectra were recorded on a Bruker ultrafleXtreme MALDI-TOF/TOF spectrometer.

Photophysical Measurements. The UV-Vis absorption spectra of all compounds in solution were obtained using a Shimadzu UV-1700 spectrophotometer in quartz cuvettes of 1 cm path-length. The emission spectra of all derivatives in solution were measured on a JASCO FP-6500 fluorescence spectrophotometer equipped with a red-sensitive WRE-343 photomultiplier tube (wavelength range: 200-850 nm).

Photocatalytic H_2 Evolution Experiments. The photocatalytic reactions were performed in 3 ml aqueous solution of TCEP/Asc (1:1) 0.1 M each at pH 5.0. The TCEP and Asc are both serving as reversible sacrificial electron donors. In all experiments 10 mg of the photosensitizer was used. The appropriate amount of catalyst was added in the reaction vessel from a stock solution of each Ni catalyst dissolved in the aprotic polar solvent DMSO. A 10 ml flask was used with a rubber septum where the mixture was purged with nitrogen for 15 min in order to remove oxygen. The reaction mixture was continuously stirred with irradiated with a 100 W white led emitting lamp. At certain time intervals 100 μl was removed from the headspace of the flask and was analyzed by Shimadzu GC 2010 plus chromatograph with a TCD detector and a molecular sieve 5 Å column (30 m - 0.53 mm) in order to measure the amount of H_2 that was produced. The H_2 amount produced was quantified using a calibration curve and in all cases, the reported H_2 production and the Turn Over Number (TON) is the average of three independent experiments.

Acknowledgements

This research was funded by the General Secretariat for Research and Technology (GSRT) and Hellenic Foundation for Research and Innovation (HFRI; project code: 508). This research has also been co-financed by the European Union and Greek national funds through the Operational Program Competitiveness, Entrepreneurship, and Innovation, under the call RESEARCH− CREATE−INNOVATE (project code: T1EDK-01504). In addition, this research has been co-financed by the European Union and Greek national funds through the Regional Operational Program “Crete 2014-2020,” project code OPS:5029187. Moreover, the European Commission’s Seventh Framework Program (FP7/2007-2013) under grant agreement no. 229927 (FP7-REGPOT-2008-1, Project BIO-SOLENUTI) and the Special Research Account of the University of Crete are gratefully acknowledged for the financial support of this research. The authors gratefully acknowledge financial support of this work by the French National Research Agency (ANR-19- CE05_0030_01).

Keywords: carbon dots • nickel catalyst • hydrogen production • photocatalysis • solar energy

[1] J. A. Turner, *Science* **2004**, *305*, 972-974.

[2] M. G. Walter, E. L. Warren, J. R. McKone, S. W. Boettcher, Q. Mi, E. A. Santori, N. S. Lewis, *Chemical Reviews* **2010**, *110*, 6446-6473.

[3] H. Furukawa, O. M. Yaghi, *Journal of the American Chemical Society* **2009**, *131*, 8875-8883.

[4] S. Chu, A. Majumdar, *Nature* **2012**, *488*, 294-303.

[5] K. Ladomenou, M. Natali, E. Iengo, G. Charalampidis, F. Scandola, A. G. Coutsolelos, *Coordination Chemistry Reviews* **2015**, *304*, 38-54.

[6] A. J. Esswein, D. G. Nocera, *Chemical Reviews* **2007**, *107*, 4022-4047.

[7] D. G. Nocera, *Accounts of Chemical Research* **2012**, *45*, 767-776.

[8] M. Han, S. Zhu, S. Lu, Y. Song, T. Feng, S. Tao, J. Liu, B. Yang, *Nano Today* **2018**, *19*, 201-218.

[9] C. Hu, M. Li, J. Qiu, Y.-P. Sun, *Chemical Society Reviews* **2019**, *48*, 2315-2337.

[10] G. A. M. Hutton, B. C. M. Martindale, E. Reisner, *Chemical Society Reviews* **2017**, *46*, 6111-6123.

[11] H. Luo, Q. Guo, P. Á. Szilágyi, A. B. Jorge, M.-M. Titirici, *Trends in Chemistry* **2020**, *2*, 623-637.

[12] K. Ladomenou, G. Landrou, G. Charalambidis, E. Nikoloudakis, A. G. Coutsolelos, *Sustainable Energy & Fuels* **2021**, *5*, 449-458.

[13] B. C. M. Martindale, G. A. M. Hutton, C. A. Caputo, E. Reisner, *Journal of the American Chemical Society* **2015**, *137*, 6018-6025.

[14] P. Du, R. Eisenberg, *Energy & Environmental Science* **2012**, *5*, 6012-6021.

[15] T. R. Simmons, G. Berggren, M. Bacchi, M. Fontecave, V. Artero, *Coordination Chemistry Reviews* **2014**, *270-271*, 127-150.

[16] P. Zhang, M. Wang, Y. Yang, T. Yao, L. Sun, *Angewandte Chemie International Edition* **2014**, *53*, 13803-13807.

[17] H. I. Karunadasa, C. J. Chang, J. R. Long, *Nature* **2010**, *464*, 1329-1333.

[18] J. L. Dempsey, B. S. Brunschwig, J. R. Winkler, H. B. Gray, *Accounts of Chemical Research* **2009**, *42*, 1995-2004.

[19] W. J. Shaw, M. L. Helm, D. L. DuBois, *Biochimica et Biophysica Acta (BBA) - Bioenergetics* **2013**, *1827*, 1123-1139.

[20] G. Landrou, A. A. Panagiotopoulos, K. Ladomenou, A. G. Coutsolelos, *Journal of Porphyrins and Phthalocyanines* **2016**, *20*, 534-541.

[21] T. Lazarides, M. Delor, I. V. Sazanovich, T. M. McCormick, I. Georgakaki, G. Charalambidis, J. A. Weinstein, A. G. Coutsolelos, *Chemical Communications* **2014**, *50*, 521-523.

[22] A. Panagiotopoulos, K. Ladomenou, D. Sun, V. Artero, A. G. Coutsolelos, *Dalton Transactions* **2016**, *45*, 6732-6738.

[23] V. Artero, M. Chavarot-Kerlidou, M. Fontecave, *Angewandte Chemie International Edition* **2011**, *50*, 7238-7266.

[24] M. Yin, S. Ma, C. Wu, Y. Fan, *RSC Advances* **2015**, *5*, 1852-1858.

[25] M. Wang, L. Chen, L. Sun, *Energy & Environmental Science* **2012**, *5*, 6763-6778.

[26] R. Jain, A. A. Mamun, R. M. Buchanan, P. M. Kozlowski, C. A. Grapperhaus, *Inorganic Chemistry* **2018**, *57*, 13486-13493.

[27] T. Straistari, J. Fize, S. Shova, M. Réglier, V. Artero, M. Orio, *ChemCatChem* **2017**, *9*, 2262-2268.

[28] M. Papadakis, A. Barrozo, T. Straistari, N. Queyriaux, A. Putri, J. Fize, M. Giorgi, M. Réglier, J. Massin, R. Hardré, M. Orio, *Dalton Transactions* **2020**, *49*, 5064-5073.

[29] S. Gulati, O. Hietsoi, C. A. Calvary, J. M. Strain, S. Pishgar, H. C. Brun, C. A. Grapperhaus, R. M. Buchanan, J. M. Spurgeon, *Chemical Communications* **2019**, *55*, 9440-9443.

[30] W.-X. Jiang, Z.-L. Xie, S.-Z. Zhan, *Inorganic Chemistry Communications* **2019**, *102*, 5-9.

[31] A. Z. Haddad, B. D. Garabato, P. M. Kozlowski, R. M. Buchanan, C. A. Grapperhaus, *J Am Chem Soc* **2016**, *138*, 7844-7847.

[32] T. Straistari, R. Hardré, J. Massin, M. Attolini, B. Faure, M. Giorgi, M. Réglier, M. Orio, *European Journal of Inorganic Chemistry* **2018**, *2018*, 2259-2266.
[33] T. Straistari, R. Hardré, J. Fize, S. Shova, M. Giorgi, M. Réglier, V. Artero, M. Orio, *Chemistry – A European Journal* **2018**, *24*, 8779-8786.
[34] A. Z. Haddad, S. P. Cronin, M. S. Mashuta, R. M. Buchanan, C. A. Grapperhaus, *Inorganic Chemistry* **2017**, *56*, 11254-11265.
[35] S. Blanchard, F. Neese, E. Bothe, E. Bill, T. Weyhermüller, K. Wieghardt, *Inorganic Chemistry* **2005**, *44*, 3636-3656.
[36] S. Panagiotakis, G. Landrou, V. Nikolaou, A. Putri, R. Hardré, J. Massin, G. Charalambidis, A. G. Coutsolelos, M. Orio, *Frontiers in Chemistry* **2019**, *7*.
[37] C. A. Calvary, O. Hietsoi, D. T. Hofsommer, H. C. Brun, A. M. Costello, M. S. Mashuta, J. M. Spurgeon, R. M. Buchanan, C. A. Grapperhaus, *European Journal of Inorganic Chemistry* **2021**, *2021*, 267-275.
[38] T. Straistari, A. Morozan, S. Shova, M. Réglier, M. Orio, V. Artero, *European Journal of Inorganic Chemistry* **2020**, *2020*, 4549-4555.
[39] M. Drosou, F. Kamatsos, C. A. Mitsopoulou, *Inorganic Chemistry Frontiers* **2020**, *7*, 37-71.
[40] M. J. M. Campbell, *Coordination Chemistry Reviews* **1975**, *15*, 279-319.
[41] N. Coutard, N. Kaeffer, V. Artero, *Chemical Communications* **2016**, *52*, 13728-13748.
[42] D. L. DuBois, *Inorganic Chemistry* **2014**, *53*, 3935-3960.
[43] R. S. Khnayzer, V. S. Thoi, M. Nippe, A. E. King, J. W. Jurss, K. A. El Roz, J. R. Long, C. J. Chang, F. N. Castellano, *Energy & Environmental Science* **2014**, *7*, 1477-1488.
[44] F. Lucarini, D. Bongni, P. Schiel, G. Bevini, E. Benazzi, E. Solari, F. Fadaei-Tirani, R. Scopelliti, M. Marazzi, M. Natali, M. Pastore, A. Ruggi, *ChemSusChem* **2021**, *14*, 1874-1885.
[45] M. Nippe, R. S. Khnayzer, J. A. Panetier, D. Z. Zee, B. S. Olaiya, M. Head-Gordon, C. J. Chang, F. N. Castellano, J. R. Long, *Chemical Science* **2013**, *4*, 3934-3945.
[46] S. Schnidrig, C. Bachmann, P. Müller, N. Weder, B. Spingler, E. Joliat-Wick, M. Mosberger, J. Windisch, R. Alberto, B. Probst, *ChemSusChem* **2017**, *10*, 4570-4580.
[47] Y. Sun, J. Sun, J. R. Long, P. Yang, C. J. Chang, *Chemical Science* **2013**, *4*, 118-124.
[48] D. Briggs, *Surface Analysis of Polymers by XPS and Static SIMS*, Cambridge University Press, Cambridge, **1998**.
[49] K. Kishi, K. Hirai, T. Yamamoto, *Surface Science* **1993**, *290*, 309-318.
[50] X. Kong, D. Castarède, A. Boucly, L. Artiglia, M. Ammann, T. Bartels-Rausch, E. S. Thomson, J. B. C. Pettersson, *The Journal of Physical Chemistry C* **2020**, *124*, 5263-5269.
[51] W. Shenglong, W. Fosong, G. Xiaohui, *Synthetic Metals* **1986**, *16*, 99-104.
[52] B. C. M. Martindale, G. A. M. Hutton, C. A. Caputo, S. Prantl, R. Godin, J. R. Durrant, E. Reisner, *Angewandte Chemie International Edition* **2017**, *56*, 6459-6463.
[53] A. Barrozo, M. Orio, *RSC Advances* **2021**, *11*, 5232-5238.

Table of Contents

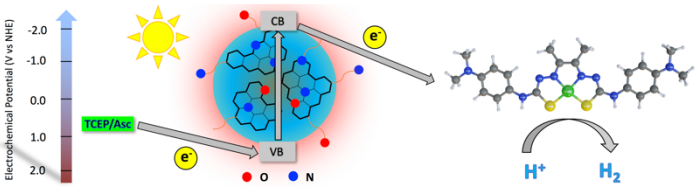

A noble metal-free photocatalytic system was designed by combining nitrogen-doped carbon dots as photosensitizers and a dimethylamino-thiosemicarbazone nickel catalyst. This promising system is shown to photoinduce hydrogen production (TON_{CAT} = 148) upon irradiation in aqueous medium.

Institute and/or researcher Twitter usernames: Maylis Orio@orio52503713